Journal of Solid State Chemistry **166,** 7–14 (2002)
doi:10.1006/jssc.2002.9543, available online at http://www.idealibrary.com on IDEAL®

Different $[Bi_{12}O_{14}]_n$ Columnar Structural Types in the Bi–Mo–Cr–O System: Synthesis, Structure, and Electrical Properties of the Solid Solution $Bi_{26}Mo_{10-x}Cr_xO_{69}$

P. Bégué,[1] J. M. Rojo, J. E. Iglesias, and A. Castro[2]

Instituto de Ciencia de Materiales de Madrid, CSIC, Cantoblanco, 28049 Madrid, Spain

Received July 31, 2001; in revised form February 5, 2002; accepted February 15, 2002

In order to search for new ionic conductor materials exhibiting a columnar $[Bi_{12}O_{14}]$ structural type, the syntheses of the solid solutions $Bi_2Mo_{1-x}Cr_xO_6$ and $Bi_{26}Mo_{10-x}Cr_xO_{69}$ have been undertaken. Single phases were obtained for the last composition with $0 \leq x \leq 5$ homogeneity range. Moreover, a new oxide with $Bi_6Cr_2O_{15}$ composition has been obtained from the limit nominal stoichiometries Bi_2CrO_6 and $Bi_{26}Cr_{10}O_{69}$. X-ray powder diffraction studies have shown that this oxide crystallizes in the orthorhombic system, space group *Ccc*2 or *Cccm*, with unit-cell parameters $a = 19.8986(9)$ Å, $b = 12.2756(6)$ Å, $c = 5.8868(3)$ Å, and $V = 1437.96$ Å^3. Impedance spectroscopy measurements carried out on the representative $Bi_{26}Mo_8Cr_2O_{69}$ phase, showed that this material is a good oxygen ion conductor, in fact the best one belongs to the columnar structural type, with a conductivity as high as 1.7×10^{-3} S cm^{-1} at 425 °C. © 2002 Elsevier Science (USA)

Key Words: **Bismuth; molybdenum; chromium; substitution; oxides; solid solution; ionic conductivity.**

INTRODUCTION

In the last few years intensive research work has been undertaken on a new bismuth-based mixed oxide family, showing a characteristic columnar $[Bi_{12}O_{14}]_n$ arrangement, because of its potentially good ionic conductivity properties. The high-temperature polymorph of the compound Bi_2MoO_6, the phase γ(H), was the first oxide belonging to this columnar structural type to be described. Its structure was solved by neutron powder diffraction by Buttrey *et al.* (1) and then refined using single crystal X-ray diffraction data (2). The framework of this oxide is built up from $[Bi_{12}O_{14}]$ columns surrounded by $[Bi_2Mo_2O_{10}]$ and $[BiMo_3O_{12}]$ units extending along one prominent crystallographic direction (Fig. 1a). Both $[Bi_2Mo_2O_{10}]$ and $[BiMo_3O_{12}]$ units are composed of one type of bismuth atom linked to MoO_4 non-condensed tetrahedra (2). Recently, the existence and structural study of the solid solutions $Bi_{2-x}Sb_xMoO_6$ $(0 \leq x \leq 0.9)$ and $Bi_{2-y}As_yMoO_6$ $(0 \leq y \leq 0.4)$, belonging to this structural type have been reported (3). Moreover, a mechanism of substitution of isovalent Sb^{3+} and As^{3+} lone-pair active cations for Bi^{3+} has been proposed for this structure (2–4).

In general, two facts have been established with regard to γ(H)-Bi_2MoO_6 type columnar oxides: (i) different iso- or aliovalent cations possessing a stereochemically active lone pair of electrons can substitute for bismuth, and (ii) these materials exhibit an interesting electrical behavior which can be improved by bismuth doping (3).

Another oxide family showing a structure with the same $[Bi_{12}O_{14}]$ columns corresponds to the general formula $Bi_{26}M_{10}O_{68+\delta}$, where M = tetrahedral cation. It was first reported by Vannier *et al.* (5) in the solid solution $Bi_{26}Mo_{10-x}V_xO_{69-x/2}$, where the structures of representative $x = 0$ and 4 terms were solved by X-ray single crystal (5, 6) and neutron and X-ray powder diffraction methods (7). In this case, the $[Bi_{12}O_{14}]$ infinite columns are separated by $[BiMo_4O_{16}]$ entities, in a similar way as in γ(H)-Bi_2MoO_6 and, unlike this one, isolated MO_4 tetrahedra (Fig. 1b). Several authors have reported the substitution of Te^{4+} and Pb^{2+} for Bi^{3+} in these oxides (8–10) and the possible location of different M cations (Mo^{6+}, W^{6+}, V^{5+}, Ge^{4+}, Al^{3+}, etc.) in the tetrahedral positions (10, 11).

Although a widespread controversy over the oxygen content of the $Bi_{26}M_{10}O_{68+\delta}$ phases (12) has attracted considerable attention on these oxides, their main merit would appear to be centered on their important electrical properties (5, 10, 11, 13). By way of example, $Bi_{26-x}Te_xMo_{8-x}V_{1+x}O_{68}$ materials exhibit conductivities as high as 10^{-2} S cm^{-1} at 700°C, independent of the structural differences for each x value.

In view of this, it seems interesting to search for new phases belonging to the columnar $[Bi_{12}O_{14}]$ structural type

[1] Present address: Civil Engineering Department, Sherbrooke University, Sherbrooke Québec Canada, J1K 2R1.

[2] To whom correspondence should be addressed. Fax: + 34 91 372 06 23. E-mail: acastro@icmm.csic.es.

0022-4596/02 $35.00

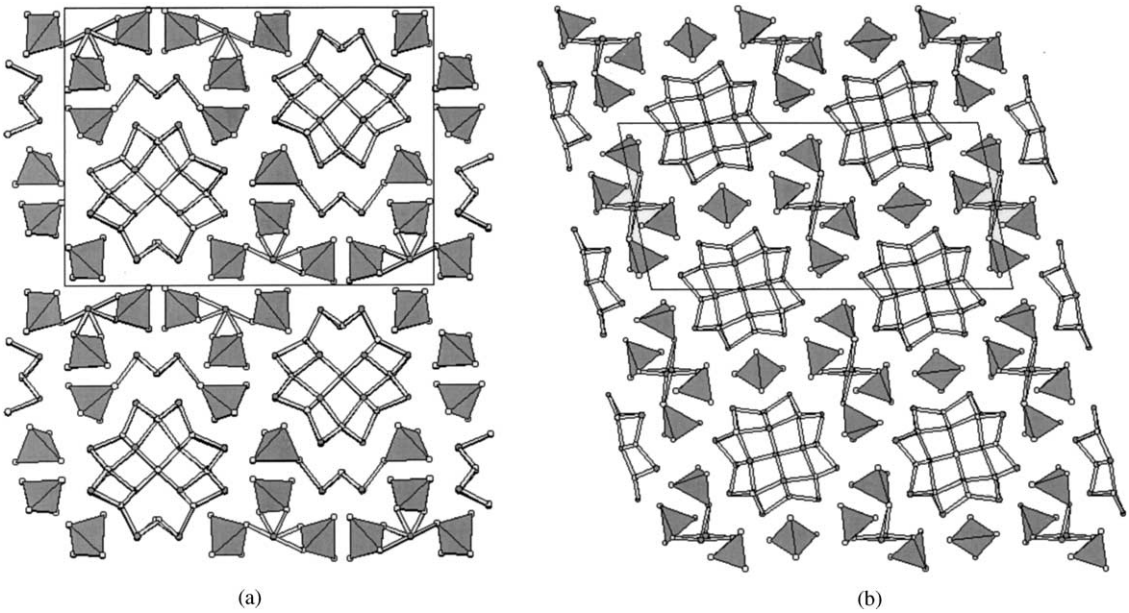

FIG. 1. Projections of: (a) γ(H)-Bi_2MoO_6 structure on (001) and (b) $Bi_{26}Mo_8V_2O_{68}$ structure on (010). Represented Bi–O bonds are ≤ 2.5 Å.

with the aim of improving the electrical response of these materials. So, the authors have undertaken the study of the possible solid solutions $Bi_2Mo_{1-x}Cr_xO_6$ and $Bi_{26}Mo_{10-x}Cr_xO_{69}$, taking into account the fact that Cr^{6+} can adopt a tetrahedral coordination like that of Mo^{6+} in these structures. This article reports on the new phases obtained, as well as their structural characterization and electrical properties.

While this paper was being written, the authors became acquainted with the structural and electrical study carried out by Grins *et al.* on $Bi_6Cr_2O_{15}$ oxide (14). This new phase also exhibits a columnar $[Bi_{12}O_{14}]$ structure, different from those previously reported, which can be considered as the simplest case in the whole family, with columns only surrounded by isolated CrO_4 tetrahedra. On the other hand, $Bi_6Cr_2O_{15}$ has a maximum electrical conductivity more than two orders of magnitude lower than the $Bi_{26}M_{10}O_{68+\delta}$ phases.

EXPERIMENTAL

Samples of about 3 g each, with nominal compositions $Bi_2Mo_{1-x}Cr_xO_6$ and $Bi_{26}Mo_{10-x}Cr_xO_{69}$, were obtained by conventional solid-state reaction from stoichiometric mixtures of Bi_2O_3, MoO_3 and CrO_3 of analytical grade. The mixtures, previously ground in an agate mortar, were heated at increasing temperatures from 400 to 800°C, for periods of 12 h. Quenching at room temperature ended thermal treatments.

The evolution of the reactions was followed by X-ray powder diffraction on a Siemens Kristalloflex 810 generator and a D-501 goniometer equipped with a graphite monochromator to select the Cu$K\alpha$ radiation ($\lambda = 1.5418$ Å). Data were recorded between 5 and 65° (2θ) with increments of 0.05° (2θ) and counting time of 2 s per step. Unit-cell parameters of the different phases were refined using the Rietveld method (15) with $Bi_{13}Mo_4VO_{34}$ (6) as structural model.

The diffractometer trace of the Bi–Cr–O_2 preparation, $5° \leq 2\theta \leq 99°$, was measured at 22°C in a Philips X'pert diffractometer, fitted with a Ge(111) incident beam monochromator of the Johansson symmetric type, using Cu$K\alpha_1$ radiation ($\lambda = 1.5405981$ Å). Previous data indicated that strain-free, well-crystallized materials could show FWHM values around 0.06°, using moderate values of the equatorial divergence. The data were therefore taken with a 0.5° divergence slit, an antiscatter slit of 1°, a receiving slit of 0.01°, and a set of Soller slits with an axial divergence of $\approx 1.1°$ in the diffracted beam path. The usual $\theta/2\theta$ mode was used, and intensity was counted at steps of 0.02° for 15 s. The flat sample was spun around its normal at about 2 Hz. A second trace was obtained under the same conditions and reduced 2θ domain, with a small amount of NIST Si standard ($a = 5.430940$ Å for the wavelength quoted above) mixed with the sample material, for calibration purposes. Peak positions were determined by hand, with the help of the diffractometer standard software.

The thermal stability of isolated phases was studied by thermogravimetric (TG) and differential thermal analysis (DTA). TG and DTA curves were recorded up to 800 °C on a Seiko 320 instrument at a heating/cooling rate of $10°C\,min^{-1}$. About 10 mg of sample were used for each run, with Al_2O_3 used as reference material.

The X-ray photoelectron spectroscopy was performed in an ultra-high-vacuum system with a base pressure of 1×10^{-10} mbar, using a double-pass cylindrical mirror analyzer. The XPS measurements were taken using Mg$K\alpha$ radiation and a pass energy of 50 eV. The surface was subjected to low argon ion beam sputter etching (1 mm A, 1 keV, 5 min).

Electrical conductivity measurements of representative $Bi_{26}Mo_8Cr_2O_{69}$ were carried out by complex impedance spectroscopy with a 1174 Solartron frequency response analyzer coupled to a 1286 Solartron electrochemical interface. Pellets of about 14 mm diameter and 1 mm thickness were prepared by cold pressing of a mechanically activated powder mixture with the composition: $13Bi_2O_3$:$8MoO_3$:$2CrO_3$. To form the phase, the pellets were heated at 700°C during 12 h and slowly cooled to room temperature. This synthesis method was employed to improve the ceramic quality, as it has been shown for other materials (16, 17). The formed phases and crystallinity were studied by X-ray powder diffraction. Platinum electrodes were deposited on the two faces by sputtering, and measurements were carried out in the temperature range 200–650°C, at steady temperatures, with pellets under airflow. The frequency range was $1–10^5$ Hz.

RESULTS AND DISCUSSION

With the aim of verifying the possible substitution of chromium VI for molybdenum VI in Bi_2MoO_6, we prepared various mixtures in different Bi_2O_3:$(1-x)MoO_3$:$xCrO_3$ ($0 \le x \le 1$) ratios and fired them, as described in the experimental part of this paper. The X-ray powder diffraction patterns of the prepared samples after the last heating at 800°C are plotted in Fig. 2. During the different heatings, no significant weight loss or gain was noted. All samples are red–brown, their color darkening with increasing chromium content, except for the sample for the $x = 1$ (all chromium) which is olivaceous green.

At first sight, three different types of phase mixtures are obtained, depending on the substitution rate. For $x = 0.1$, γ(H)-Bi_2MoO_6 is the major phase obtained. For $x = 0.25$ to 0.75, another type of phase mixture appears. Comparing the X-ray diffraction patterns of the $x = 0.5$ sample and that of the $Bi_{26}Mo_8V_2O_{68}$ columnar structure type phase (Fig. 3), it appears that the dominant phase obtained for this substitution range is this $Bi_{26}M_{10}O_{68+\delta}$ columnar type phase. Finally, the $x = 1$ pattern shows a phase mixture in which some components cannot be identified.

If we assume that all bismuth and molybdenum oxides are used up in the formation of the columnar phases, the chemical reactions can be formulated as follows:

$$x = 0.25, \quad 13Bi_2O_3 + 39/4MoO_3 + 13/4CrO_3 \rightarrow Bi_{26}Mo_{9.75}Cr_{0.25}O_{69} + 3CrO_x,$$

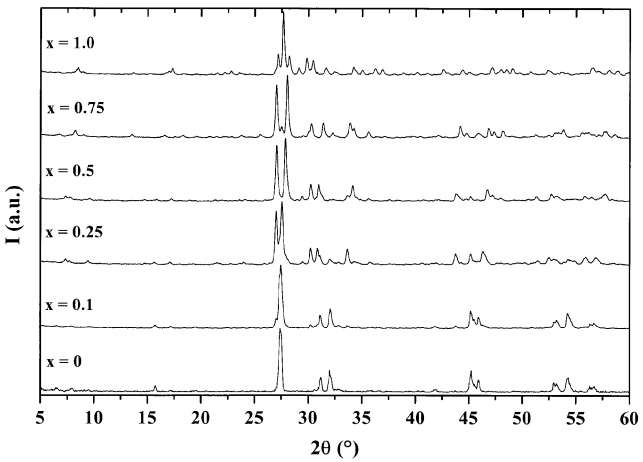

FIG. 2. X-ray diffraction patterns of Bi_2O_3:$(1-x)MoO_3$:$xCrO_3$ ($0 \le x \le 1$) after the last heating at 800°C.

$$x = 0.5, \quad 13Bi_2O_3 + 13/2MoO_3 + 13/2CrO_3 \rightarrow Bi_{26}Mo_{6.5}Cr_{3.5}O_{69} + 3CrO_x,$$

$$x = 0.75, \quad 13Bi_2O_3 + 13/4MoO_3 + 39/4CrO_3 \rightarrow Bi_{26}Mo_{3.25}Cr_{6.75}O_{69} + 3CrO_x.$$

However, no particular chromium oxide could be identified in the X-ray diffraction patterns, which is the reason for the notation CrO_x employed hereinafter.

Thus, in view of the feasibility of forming the $Bi_{26}Mo_{10-x}Cr_xO_{69}$ phases, we set out to ascertain the existence of such a solid solution with a columnar structure type, through the preparation of various $13Bi_2O_3$:$(10-x)$ MoO_3:$xCrO_3$ ($0 \le x \le 10$) samples. The X-ray powder diffraction patterns of the different prepared mixtures after the final heating are plotted in Fig. 4, together with the $Bi_{26}Mo_8V_2O_{68}$ pattern as reference. For x ranging from

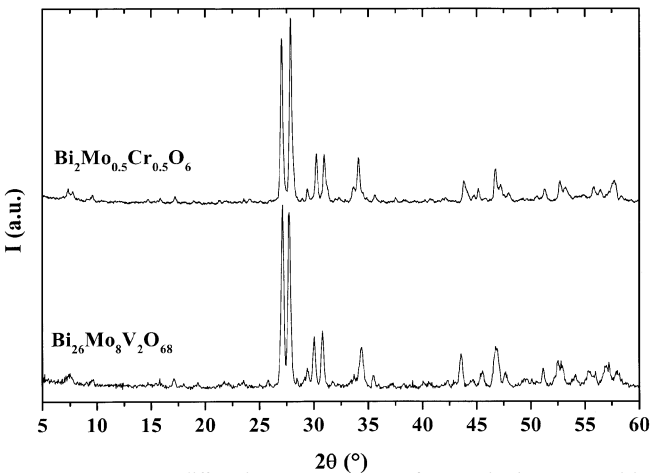

FIG. 3. X-ray diffraction patterns of nominal composition $Bi_2Mo_{0.5}Cr_{0.5}O_6$ and $Bi_{26}Mo_8V_2O_{68}$ oxide.

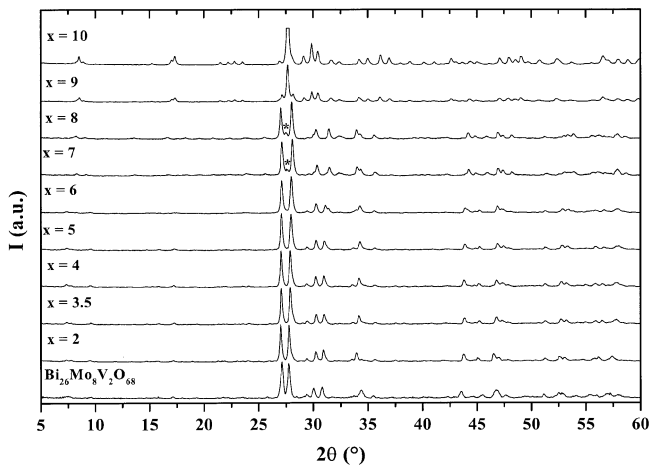

FIG. 4. X-ray diffraction patterns of $13Bi_2O_3$:$(10-x)MoO_3$:$xCrO_3$ ($0 \le x \le 10$) after the last heating. The asterisk marks the onset of the $Bi_6Cr_2O_{15}$ phase.

0 to 5, single phases with the columnar $Bi_{26}M_{10}O_{68+\delta}$ structure type are obtained. From $x = 6$ to 8, those phases are mixed with other phases that could not be identified, and these become predominant for the last two compositions ($x = 9$ and 10). Also in this case, no weight loss or gain was noted during the different heating. All samples are orange, darkening to red–brown with increasing chromium content, except the all-chromium one which is dark green.

In order to determine the limits of this new solid solution, the unit-cell parameters were refined by the Rietveld method, using the $Bi_{26}Mo_8V_2O_{68}$ structure as a model, with satisfactory reliability factors. The evolution of the unit-cell parameters versus composition is plotted in Fig. 5. All parameters underwent a regular decrease to $x = 5$, but from $x = 5$ to 6, the a, c and β parameters increase whilst b still decreases. In consequence, the upper limit of the solid solution can be fixed at around $x = 5$. This general decrease of all unit-cell parameters can be expected, since a larger cation is being substituted for by a smaller one [$r_{Mo^{6+}} = 0.41$ Å and $r_{Cr^{6+}} = 0.26$ Å (18)].

Finally, if we compare the reacted mixtures having the nominal compositions Bi_2CrO_6 and $Bi_{26}Cr_{10}O_{69}$, it can be seen that their X-ray patterns are identical. This fact should imply that we are here in front of a new phase. Recently, some authors (14) reported the existence of a new bismuth–chromium phase, $Bi_6Cr_2O_{15}$ with columnar structure. Taking into account these data, we can then write the following reactions:

$$Bi_2CrO_6, \qquad 3Bi_2O_3 + 3CrO_3 \rightarrow Bi_6Cr_2O_{15} + CrO_x,$$

$$Bi_{26}Cr_{10}O_{69}, \quad 13Bi_2O_3 + 10CrO_3 \rightarrow 13/3Bi_6Cr_2O_{15} + 4/3CrO_x.$$

In these cases, the phase is also obtained with different chromium oxides which have not been identified.

In order to study this new phase, the first 25 reflections of a diffractometer trace, taken under high-resolution

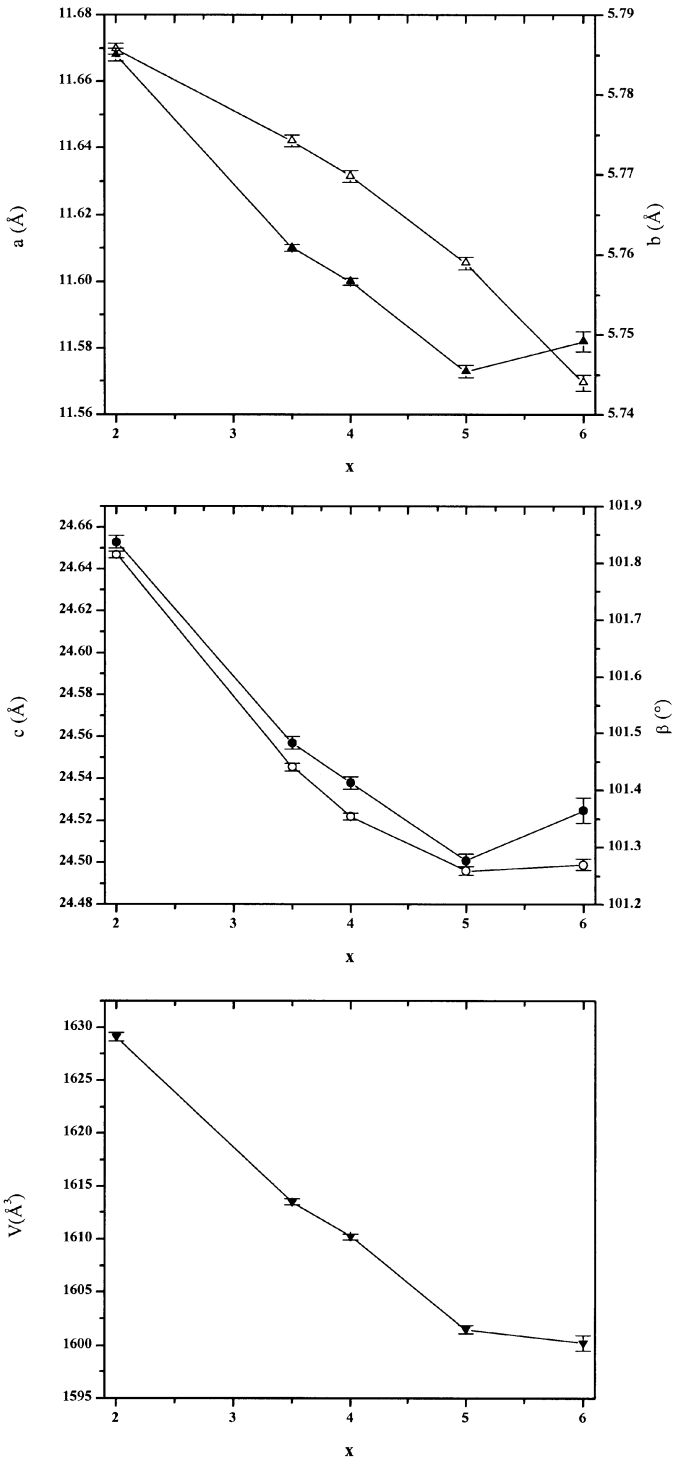

FIG. 5. Evolution of unit-cell parameters with composition for the solid solution $Bi_{26}Mo_{10-x}Cr_xO_{69}$. The black symbols correspond to the scale on the left-hand side of the figures.

conditions (see experimental section), were indexed with TREOR (19) after correction of the four lowest angle Bragg peaks with values obtained from their higher orders (4th for the first one, and 2nd for the other three). An orthorhombic cell with $a = 19.884$ Å, $b = 12.259$Å, $c = 5.883$ Å, was found which appeared to be a good candidate [all 25 lines indexed, M_{20} (20) = 34] for further analysis. The lattice parameters were then refined by a least-squares procedure using 75 observed lines up to $2\theta = 60°$. As the refinement advanced it became evident that the lattice was C-centered (the Miller indices satisfied the selection rule: hkl, $h + k = 2n$) so four weak lines not satisfying the rule (intensities $< 1\%$ for three of them, 1.7% for the fourth one) were excluded from the refinement, and labeled as impurity lines. The final parameters obtained for the C-lattice of this compound were $a = 19.8986(9)$ Å, $b = 12.2756(6)$ Å, $c = 5.8868(3)$ Å and $V = 1437.96$ Å^3, with $|2\theta_{obs} - 2\theta_{cal}| \leq 0.025°$ for all observations. The Niggli cell has parameters $a = 11.6902(4)$ Å, $b = 5.8868(3)$ Å, $c = 11.6902(4)$ Å, $\beta = 116.658(2)°$. The final reliability estimators for this indexing were $M_{20} = 87$, ($\langle\varepsilon\rangle = 0.000015$, 28); $M_{40} = 39$, ($\langle\varepsilon\rangle = 0.000028$, 63); $M_{70} = 25$, ($\langle\varepsilon\rangle = 0.000036$, 139). From the indexed lines, two further sets of systematic absences were noted: $0\,k\,l$, $l = 2n$ ($k = 2n$); $h\,0\,l$, $l = 2n$ ($h = 2n$); just a single observation (intensity 2.2%, with Miller indices 001) stood in violation of these. If this weak line is also considered an impurity line, the possible space group could be either *Ccc*2 (No. 37) or *Cccm* (No. 66). We carried out an independent indexing process with a different algorithm implemented in program DICVOL91 (21), using the first 20 observed reflections. The result was the same orthorhombic solution as given above, with $M_{20} = 25$, $F_{20} = 45$, plus three more monoclinic cells having exactly the same volume as the first one, which turned out to be different descriptions of the same lattice. The indexed X-ray powder diffraction pattern of $Bi_6Cr_2O_{15}$ is reported in Table 1.

The crystal data for the phase agrees well with that reported for $Bi_6Cr_2O_{15}$ by Grins *et al.* (14). The differences are $< 0.2\%$ in all parameters, but still these differences represent more than 10 standard deviations, which is understandable, since these authors have measured a pure phase, while ours may have some small amount of chromium in solid solution.

Thermal analysis undertaken on all single phases under airflow reveal their stability between room temperature and 800°C.

As all $Bi_{26}Mo_{10-x}Cr_xO_{69}$ single phases present an orange color and no weight variation was observed, it can reasonably be thought that the chromium cation had conserved its VI oxidation state, despite having been heated at high temperature. In order to verify this assumption, an X-ray photoelectron spectroscopy (XPS) experiment was undertaken on the $x = 2$ sample. In Fig. 6, the obtained spectra for each species before and after laser abrasion are plotted. In this phase, bismuth ion presents its classical III oxidation state as revealed by the binding energy observed ($E_B = 159.7$ eV to be compared with 159.6 and 159.8 eV for Bi_2MoO_6 and $Bi_2Mo_2O_9$, respectively). Molybdenum also conserves its VI oxidation state ($E_B = 232.2$, 232.7 eV for MoO_3). Concerning chromium, the observed binding energy value of 579.6 eV, compared with 580.1 and 576.6 eV for CrO_3 and Cr_2O_3, respectively, clearly indicates that in this sample chromium cations are present in the form of Cr^{6+}. This experiment allows us to confirm the previous formulation of this new solid solution as $Bi_{26}Mo_{10-x}Cr_xO_{69}$.

Impedance measurements were carried out on $Bi_{26}Mo_8Cr_2O_{69}$ between 200 and 700°C, in steps of 25°C. A typical impedance plot is shown in Fig. 7. Two arcs and one spike are observed. On heating, the arcs disappear gradually and the spike is better observed. The high-frequency arc is ascribed to the grain interior response but its

TABLE 1
X-Ray Powder Diffraction Pattern (22°C) for Orthorhombic $Bi_6Cr_2O_{15}$

	h	k	l	d_{obs}	I/I_0	$2\theta_{obs}$	$2\theta_{calc}$	$\Delta 2\theta$	Comment
1	1	1	0	10.45	24	8.455	8.457	−0.002	
2	2	0	0	9.95	8	8.884	8.881	0.003	
3	0	2	0	6.14	1	14.422	14.419	0.003	
4	0	0	1	5.89	2	15.035	15.038	−0.003	impurity line (see text)
5	3	1	0	5.84	3	15.168	15.171	−0.003	
6	2	2	0	5.22	8	16.956	16.960	−0.004	
7	1	1	1	5.13	15	17.270	17.276	−0.006	
8	3	1	1	4.15	3	21.415	21.423	−0.008	
9	1	3	0	4.01	3	22.163	22.161	0.002	
10	2	2	1	3.908	5	22.738	22.740	−0.002	
11	4	2	0	3.864	> 1	22.996	22.994	0.002	
12	5	1	0	3.787	5	23.474	23.480	−0.006	
13	6	0	0	3.315	4	26.871	26.861	0.010	
14	4	2	1	3.231	100	27.588	27.588	0.000	
15	5	1	1	3.184	6	27.997	27.999	−0.002	

TABLE 1—*Continued*

	h	k	l	d_{obs}	I/I_0	$2\theta_{obs}$	$2\theta_{calc}$	$\Delta 2\theta$	Comment
16	0	4	0	3.068	8	29.081	29.073	0.008	
17	3	3	1	2.9973	26	29.784	29.784	0.000	
18	0	0	2	2.9440	17	30.336	30.342	−0.006	
19	6	2	0	2.9163	1	30.631	30.616	0.015	
20	5	3	0	2.8525	1	31.334	31.329	0.005	shoulder of following
21	1	1	2	2.8332	5	31.553	31.554	−0.001	
22	2	0	2	2.8232	3	31.667	31.676	−0.009	partially resolved from precedent
23	7	1	0	2.7692	4	32.302	32.300	0.002	
24	2	4	1	2.6252	6	34.126	34.130	−0.004	
25	6	2	1	2.6144	2	34.272	34.274	−0.002	shoulder of precedent
26	5	3	1	2.5669	7	34.926	34.920	0.006	
27	7	1	1	2.5063	> 1	35.798	35.804	−0.006	
28	8	0	0	2.4875	11	36.078	36.081	−0.003	
29	1	5	0	2.4360	7	36.868	36.858	0.010	
30	1	3	2	2.3726	2	37.890	37.894	−0.004	
31	4	2	2	2.3422	> 1	38.401	38.412	−0.011	
32	5	1	2	2.3233	4	38.726	38.719	0.007	
33	1	5	1	2.2507	2	40.028	40.015	0.013	
34	6	0	2	2.2018	3	40.956	40.964	−0.008	
35	7	3	1	2.1707	> 1	41.569	41.581	−0.012	
36	8	2	1	2.1455		42.082	42.060	0.022	unresolved doublet
37	3	5	1	2.1455	1	42.082	42.106	−0.024	
38	0	4	2	2.1242	7	42.524	42.522	0.002	
39	6	4	1	2.1038	3	42.957	42.958	−0.001	
40	2	4	2	2.0776	2	43.526	43.529	−0.003	partially resolved doublet
41	6	2	2	2.0728	2	43.632	43.645	−0.013	
42	5	3	2	2.0487	2	44.172	44.175	−0.003	
43	9	1	1	2.0408	3	44.351	44.347	0.004	
44	7	1	2	2.0170	2	44.904	44.904	0.000	
45	2	6	0	2.0037	> 1	45.218	45.210	0.008	
46	5	5	1	1.96872	1	46.067	46.057	0.010	
47	9	3	0	1.94503	2	46.661	46.658	0.003	
48	8	4	0	1.93202	7	46.994	46.986	0.008	
49	1	1	3	1.92800	3	47.098	47.084	0.014	shoulder of precedent
50	8	0	2	1.89992	6	47.837	47.840	−0.003	
51	1	5	2	1.87727	4	48.451	48.460	−0.009	
52	7	5	0	1.85844	9	48.974	48.985	−0.011	
53	9	3	1	1.84667	1	49.307	49.299	0.008	
54	2	2	3	1.83651	3	49.598	49.586	0.012	
55	7	3	2	1.82891	1	49.818	49.813	0.005	
56	3	5	2	1.81383	1	50.261	50.270	−0.009	
57	4	6	1	1.80140	4	50.632	50.632	0.000	
58	6	4	2	1.78874	1	51.016	51.015	0.001	
59	1	3	3	1.76233	1	51.837	51.835	0.002	
60	4	2	3	1.74961	6	52.242	52.241	0.001	
61	5	1	3	1.74242	3	52.474	52.483	−0.009	
62	3	3	3	1.70945	2	53.566	53.562	0.004	
63	12	0	0	1.65836	2	55.355	55.360	−0.005	shoulder of the following
64	2	6	2	1.65610	2	55.437	55.422	0.015	
65	9	5	0	1.64261	1	55.932	55.920	0.012	
66	3	7	1	1.62945	6	56.424	56.434	−0.010	
67	8	4	2	1.61557	3	56.953	56.961	−0.008	
68	11	3	1	1.59273	5	57.846	57.844	0.002	
69	7	5	2	1.57114	4	58.718	58.716	0.002	
70	5	7	1	1.54856		59.660	59.672	−0.012	unresolved doublet
71	12	2	1	1.54492	5	59.815	59.823	−0.008	

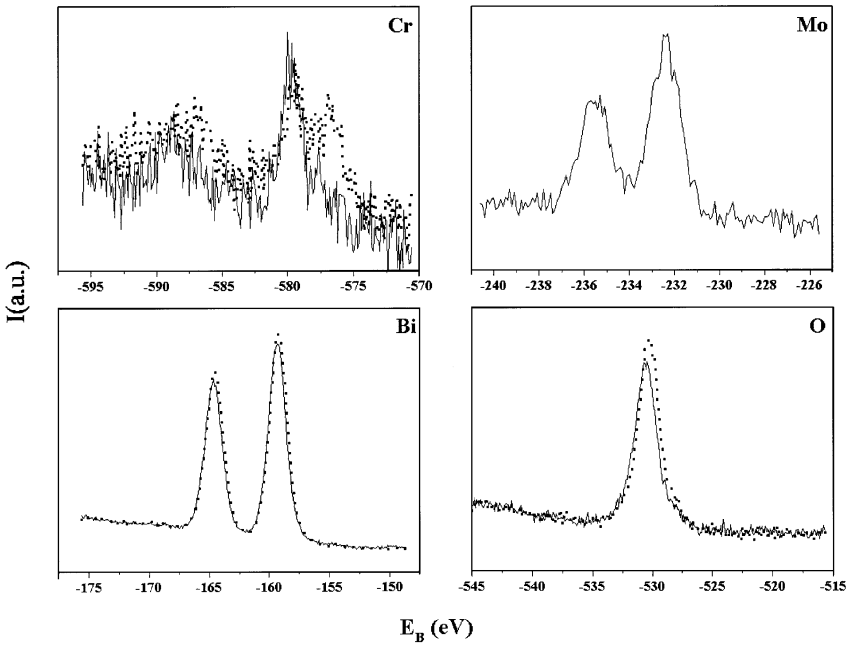

FIG. 6. XPS spectra of $Bi_{26}Mo_8Cr_2O_{69}$ phase. The continuous line represents data measured before laser abrasion.

capacitance could not be calculated because of the apparatus limitations at high frequency. The low-frequency arc shows a capacitance of 2 nF and is ascribed to the grain-boundary response. The spike is ascribed to blocking of the mobile ions (O^{2-}) at the electrodes (21). The resistance associated with the high-frequency arc was determined from the intercept of this arc with the real Z' axis, and then, the conductivity was calculated as usual. The plot of conductivity ($\log_{10}\sigma$) as a function of reciprocal temperature ($1000/T$) is given in Fig. 8. The experimental data are fitted to two straight lines with a crossover at 275°C. The activation energy values are 0.73 and 0.54 eV below and above that temperature. These energies are a little lower than those reported for oxygen ion conductors. The change observed in activation energy would be associated with an order–disorder transition (5). The maximum conductivity value reached is $1.7 \times 10^{-3}\,S\,cm^{-1}$ at 425°C.

Comparing the conductivity of $Bi_{26}Mo_8Cr_2O_{69}$ with that found in other phases exhibiting columnar type structures

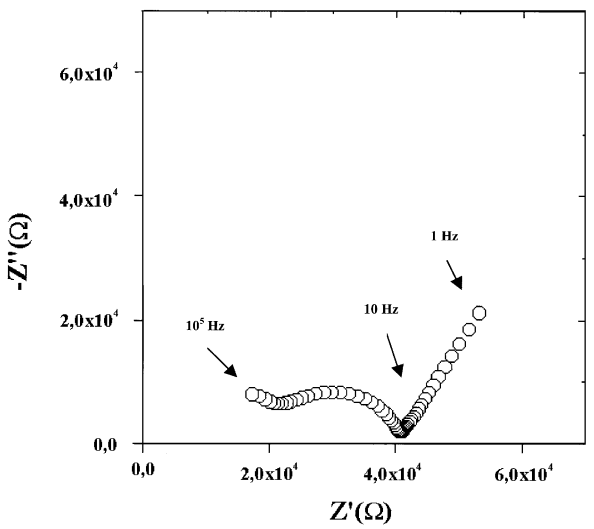

FIG. 7. Impedance plot (imaginary versus real part) recorded at 200°C for $Bi_{26}Mo_8Cr_2O_{69}$.

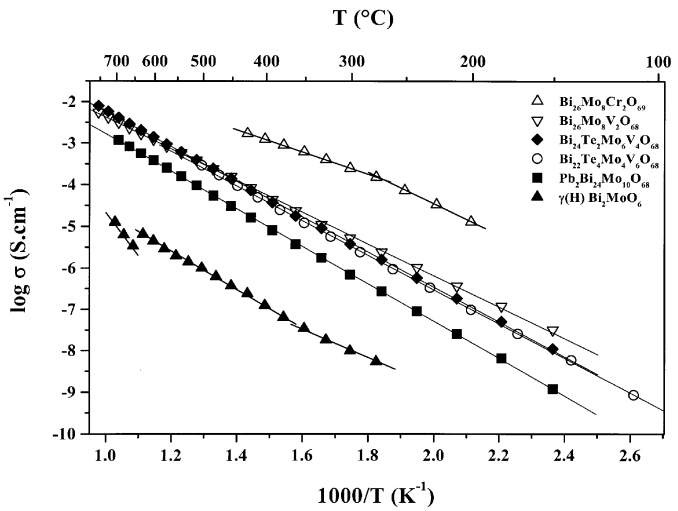

FIG. 8. Conductivity (σ) versus reciprocal temperature for $Bi_{26}Mo_8Cr_2O_{69}$ (') and other $Bi_{26}M_{10}O_{68+\delta}$ columnar structure phases.

(Fig. 8), it can be seen that this material has the highest conductivity in the temperature range studied; for example it presents a higher conductivity than that of $Bi_{26}Mo_{10}O_{69}$ at the same temperature [$\sigma(Bi_{26}Mo_{10}O_{69}) \cong 5 \times 10^{-4}\,S\,cm^{-1}$ at about 425°C (5)]. Furthermore, the arrangement of different entities surrounding the columns, that is, the different structural columnar types, seems to have a major influence on the conductivity. Thus, γ(H)-Bi_2MoO_6 and $Bi_6Cr_2O_{15}$ show very similar conductivities, which are very much lower than those reported for $Bi_{26}M_{10}O_{68+\delta}$ phases (3,14). The oxygen content of the last phases also appears as an important factor for good conductivity, as the $Bi_{26}Mo_8Cr_2O_{69}$ phase presents a higher conductivity than the $Bi_{26}M_{10}O_{68}$ ones. The presence of the extra oxygen in an interstitial position in the former structure might be responsible for the easier oxygen diffusion in the lattice.

CONCLUSIONS

Taking as starting point the columnar structural types γ(H)-Bi_2MoO_6 and $Bi_{26}M_{10}O_{68+\delta}$, the synthesis of new phases showing columns [$Bi_{12}O_{14}$] has been achieved by the substitution of isovalent Cr^{6+} for Mo^{6+} in both structures. The most complicated γ(H)-Bi_2MoO_6 structure, built up from [$Bi_{12}O_{14}$] columns surrounded by [$Bi_2Mo_2O_{10}$] and [$BiMo_3O_{12}$] units, does not admit such substitution, but nominal compositions $Bi_2Mo_{1-x}Cr_xO_6$ lead to the synthesis of new $Bi_{26}Mo_{10-x}Cr_xO_{69}$ phases, mixed with unidentified chromium oxides. A $Bi_{26}Mo_{10-x}Cr_xO_{69}$ solid solution has been isolated for x values ranging from 0 to 5. These phases show a simpler columnar arrangement with the [$Bi_{12}O_{14}$] columns this time surrounded by [$Bi(Mo,Cr)_4O_{16}$] entities and isolated $(Mo,Cr)O_4$ tetrahedra. The limit compositions without molybdenum, Bi_2CrO_6 and $Bi_{26}Cr_{10}O_{69}$, do not appear to be stable as single phases under the experimental conditions; instead we obtain in both cases the same new oxide $Bi_6Cr_2O_{15}$, mixed with chromium oxides, CrO_x.

Preliminary structural work on the new $Bi_6Cr_2O_{15}$ phase leads to the orthorhombic system, space group *Ccc*2 or *Cccm*, with unit-cell parameters $a = 19.8986(9)$ Å, $b = 12.2756(6)$ Å, $c = 5.8868(3)$ Å and $V = 1437.96$ Å^3. Very recent results by Grins *et al.* (14) indicate that this oxide also exhibits a columnar structure, the simplest one so far described, with the columns [$Bi_{12}O_{14}$] exclusively separated by CrO_4 tetrahedra.

The representative $x = 2$ member of the new solid solution, $Bi_{26}Mo_8Cr_2O_{69}$, shows the highest conductivity reported for columnar [$Bi_{12}O_{14}$] oxides, which probably correlates with the existence of extra oxygen located in interstitial positions of the framework.

In summary, this work shows how the substitution of Cr^{6+} for Mo^{6+} in columnar structural-type oxides is progressively carried out with a simplification of the structure. At the same time, the oxygen ion conduction is improved.

ACKNOWLEDGMENTS

The authors thank MCYT of Spain for financial support under project MAT2001-0561. They acknowledge fruitful discussions with Dr. E. Román (ICMM/CSIC, Spain). P.B. thanks the Spanish Government for the grant awarded.

REFERENCES

1. D. J. Buttrey, T. Vogt, U. Wilgruber, and W. R. Robinson, *J. Solid State Chem.* **111,** 118 (1994).
2. P. Bégué, R. Enjalbert, J. Galy, and A. Castro, *Solid State Sci.* **2,** 637 (2000).
3. P. Bégué, Ph. D. Thesis, Université Paul Sabatier, Toulouse, France, 2001.
4. P. Bégué, R. Enjalbert, and A. Castro, *J. Solid State Chem.* **159,** 72 (2001).
5. R. N. Vannier, G. Mairesse, F. Abraham, and G. Nowogrocki, *J. Solid State Chem.* **122,** 394 (1996).
6. R. Enjalbert, G. Hasselmann, and J. Galy, *J. Solid State Chem* **131,** 236 (1997).
7. D. J. Buttrey, T. Vogt, G. P. A. Yap, and L. Rheingold, *Mater. Res. Bull.* **32,** 947 (1997).
8. R. Enjalbert, G. Hasselmann, and J. Galy, *Acta Crystallogr. C* **53,** 269 (1997).
9. A. Castro, R. Enjalbert, P. Baules, and J. Galy, *J. Solid State Chem.* **139,** 185 (1998).
10. R. N. Vannier, S. Danzé, G. Nowogrocki, M. Huvé, and G. Mairesse, *Solid State Ion.* **136–137,** 51 (2000).
11. B. Bastide, R. Enjalbert, S. Villain, A. Castro, and J. Galy, "VIIth European Conference on Solid State Chemistry, Madrid, Spain, 1999."
12. R. N. Vannier, F. Abraham, G. Nowogrocki, and G. Mairesse, *J. Solid State Chem.* **142,** 294 (1999).
13. P. Bégué, J. M. Rojo, R. Enjalbert, J. Galy, and A. Castro, *Solid State Ion.* **112,** 275 (1998).
14. J. Grins, S. Esmaeilzadeh, and S. Hull, *J. Solid State Chem.* **163,** 144 (2002).
15. J. Rodríguez-Carbajal, Fullprof, Version 0.2, Mars 98, Laboratoire Leon Brillouin (CEA-CNRS), Saclay, France.
16. A. Castro, P. Millán, L. Pardo, and B. Jiménez, *J. Mater. Chem.* **9,** 1313 (1999).
17. L. Pardo, A. Castro, P. Millán, C. Alemany, R. Jiménez, and B. Jiménez, *Acta Mater* **48,** 2421 (2000).
18. R. D. Shannon, *Acta Crystallogr. A* **32,** 751 (1976).
19. P.-E. Werner, L. Eriksson, and M. Westdahl, *J. Appl. Cryst.* **18,** 367 (1985).
20. P.M. de Wolf, *J. Appl. Cryst.* **1,** 108 (1968).
21. A. Boultif and M. Louër, *J. Appl. Crystallogr.* **24,** 987 (1991).
22. J. R. Macdonald, "Impedance Spectroscopy, Emphasizing Solid Materials and Systems." John Wiley, New York, 1987.